arXiv:1412.0994v1 [nlin.PS] 2 Dec 2014

Breather mobility and the PN potential
Brief review and recent progress

Magnus Johansson and Peter Jason

Abstract The question whether a nonlinear localized mode (discrete soliton/breather) can be mobile in a lattice has a standard interpretation in terms of the Peierls-Nabarro (PN) potential barrier. For the most commonly studied cases, the PN barrier for strongly localized solutions becomes large, rendering these essentially immobile. Several ways to improve the mobility by reducing the PN-barrier have been proposed during the last decade, and the first part gives a brief review of such scenarios in 1D and 2D. We then proceed to discuss two recently discovered novel mobility scenarios. The first example is the 2D Kagome lattice, where the existence of a highly degenerate, flat linear band allows for a very small PN-barrier and mobility of highly localized modes in a small-power regime. The second example is a 1D waveguide array in an active medium with intrinsic (saturable) gain and damping, where exponentially localized, travelling discrete dissipative solitons may exist as stable attractors. Finally, using the framework of an extended Bose-Hubbard model, we show that while quantum fluctuations destroy the mobility of slowly moving, strongly localized classical modes, coherent mobility of rapidly moving states survives even in a strongly quantum regime.

Key words: Peierls-Nabarro potential, breather mobility, discrete flat-band solitons, discrete dissipative solitons, quantum compactons, extended Bose-Hubbard model

M Johansson
Department of Physics, Chemistry and Biology (IFM), Linköping University, SE-581 83 Linköping, Sweden e-mail: mjn@ifm.liu.se

P Jason
Department of Physics, Chemistry and Biology (IFM), Linköping University, SE-581 83 Linköping, Sweden

1 Introduction

The concept of a Peierls-Nabarro (PN) potential, and a corresponding PN barrier, to describe the motion of a localized excitation in a periodic lattice has ancient roots. It originates in the work of Peierls from 1940 [61], later expanded and corrected by Nabarro [55], calculating the minimum stress necessary for moving a dislocation in a simple cubic lattice. A classical model for describing dislocation motion is the Frenkel-Kontorova (FK), or discrete sine-Gordon, model [4], where dislocations appear as discretizations of the topological kink solitons of the continuum sine-Gordon equation. In the continuum limit, the system is Lorentz invariant so the kink can be boosted to an arbitrary velocity without energy threshold. The lattice discreteness breaks the translational invariance and singles out two possible configurations for a stationary kink: a stable configuration centered in-between two lattice sites ("bond-centered", "inter-site") and an unstable configuration centered at a lattice site ("site-centered", "on-site"). Defining the PN barrier as the minimum energy that must be added to a stable kink in order to translate it one lattice site, it becomes equal to the energy difference between the site-centered and bond-centered kinks, since the kink must pass through a site-centered configuration in order to reach its next stable lattice position. If in addition one assumes that the kink travels very slowly and adiabatically through the lattice, one may employ a collective coordinate approach using the kink center as a collective coordinate. Calculating the kink energy as a function of its center then defines a PN potential as a continuous and periodic function of the lattice position, where stable positions appear as minima and unstable positions as maxima or saddles. See Ref. [4] for more detailed discussions, and further references, concerning the PN potential for FK kinks.

It is then highly tempting to carry over a similar reasoning for describing the mobility also of nontopological lattice solitons, e.g., discrete breathers and discrete envelope and pulse solitons (cf, e.g., Refs. [8, 14]). Indeed, as we will illustrate with many examples in the remainder of this chapter, such an approach is often very useful and has lead to much progress in understanding the conditions for breather mobility in various models. However, some cautionary remarks may be in order before proceeding, in particlar for the reader more inclined towards rigorous approaches. First, as was pointed out early by Flach and Willis [30, 31], a problem arises with the definition of a PN barrier/potential for discrete breathers in generic Hamiltonian lattices, since breathers come in continuous families and typically also have internal oscillation modes which may increase or decrease their energy. Thus, strictly speaking, there is no unique minimum energy needed for translating a breather one site since it depends on the internal breather degrees of freedom, and therefore no well-defined PN barrier unless some additional constraint is imposed on the dynamics. This problem does not occur for kinks, since they carry topological charge and the stable kink is a global energy minimizer under the given boundary conditions. Second, the PN potential is defined assuming adiabatic (ideally infinitely slow) motion, and therefore the fact that a localized mode can be supplied with sufficient energy to overcome the PN barrier does not imply the existence of *exact* moving discrete solitons at *finite* (possibly large) velocities. On the contrary: a localized

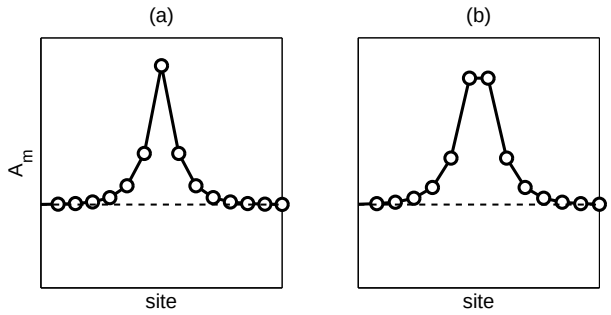


Fig. 1 Illustrations of stationary DNLS breathers: (a) on-site; (b) inter-site.

mode travelling through the periodic potential with a nonzero velocity will generate oscillations, which in the generic case will resonate with oscillation frequencies for linear waves. Thus, the motion causes radiation to be emitted, and the mode eventually slows down and/or decays. See Ref. [28] for further discussion and references on this issue, and Ref. [62] for a more mathematical approach.

As mentioned, the first problem above may be overcome by imposing some additional constraint on the dynamics. As discussed by Cretegny and Aubry [12, 2], a natural assumption would be that a breather moves at a constant total action, since for a time-periodic trajectory the action can be identified with the area inside a loop in phase space, which is conserved for any Hamiltonian system. Thus, assuming adiabatic motion with a velocity much smaller than the oscillation frequency of the breather, the action should be at least approximately conserved also for a moving breather (see also Ref. [46] for a related approach, and Ref. [67] for a tutorial review). In fact, for the very important class of Discrete Nonlinear Schrödinger (DNLS) lattices [22, 41], which will be the main focus of this chapter, this statement is even rigorously true! The action then corresponds to the total norm (which, depending on the particular physical application of the model, may correspond e.g. to power, or particle number), which is a second conserved quantity of all DNLS-type lattices. In the particular case of a "standard" 1D DNLS chain with cubic, on-site nonlinearity (Eq. (1) below with $K_4 = K_5 = 0$), it was realized by Eilbeck already in 1986 [20] (later rediscovered in Ref. [43]) that the proper definition of a PN barrier then corresponds to comparing the energy of the on-site discrete soliton (which here is stable, Fig. 1 (a)) with the (unstable, Fig. 1 (b)) inter-site soliton *at fixed norm*. He also concluded that for strong nonlinearity, corresponding to highly localized solitons, the PN barrier grows proportionally to the nonlinearity strength, and therefore such solitons cannot be moved but are pinned to the lattice. In fact, it has later also been rigorously proven that stable DNLS solitons are global energy minimizers at fixed norm [72], which justifies the definition of the PN barrier as the minimum additional energy needed for translating the ground-state soliton one lattice site in slow, adiabatic motion. A very recent work [37] has also rigorously shown that for weak nonlinearity, when the DNLS soliton approaches the continuous NLS soliton,

the PN-barrier becomes exponentially small in the discreteness parameter (lattice constant).

It should also be noted that although DNLS-type models have the non-generic property of exact norm conservation, such models generically arise in approximate, rotating-wave type, descriptions of the slow modulational, small-amplitude dynamics of more general nonlinear lattice models with anharmonic on-site (Klein-Gordon, KG) and/or intersite (Fermi-Pasta-Ulam, FPU) interactions. A separation of time-scales between fast, small-amplitude oscillations (e.g. breather frequency) and slow modulations (e.g. breather movement) is a crucial ingredience in all such approaches, see, e.g., Refs [38, 53] for discussion and further references. Thus, under these conditions, we should expect the Peierls-Nabarro potentials and barriers analyzed for DNLS models to also give good approximate descriptions of breather mobility in the corresponding KG/FPU lattices.

After this very brief general review of the basic concepts of PN potential and barrier and their relation to breather mobility, the remainder of this chapter will focus on describing various ways to improve the mobility of strongly localized modes by reducing the PN-barrier, that have been proposed during the last decade. Sec. 2 discusses briefly the one-dimensional (1D) scenario, mainly within the framework of a DNLS model extended with inter-site nonlinearities. In Sec. 3, we first give a general, short overview of different two-dimensional (2D) mobility scenarios that have been discussed in the literature, and then focus more particularly on the saturable DNLS model and the corresponding PN potential (Sec. 3.1), and the Kagome lattice with mobile "flat-band" discrete solitons (Sec. 3.2). Sec. 4 describes how an intrinsic gain may support exact localized travelling discrete dissipative solitons, and in Sec. 5 we analyze the quantum mechanical counterparts to strongly localized moving modes, and discuss the conditions under which the classical PN potential concept has a meaningful quantum counterpart.

2 PN-barriers and discrete soliton mobility in 1D

As discussed above, for the "standard" DNLS equation, with a pure on-site, cubic nonlinearity, the energy difference between the stable, site-centered mode and the unstable, bond-centered mode is always nonzero and grows with increasing nonlinearity, and therefore strongly localized modes are highly immobile. Thus, in generic cases, we should expect PN potentials and barriers to be always nonvanishing. Exceptions occur for integrable models, such as the Ablowitz-Ladik discretization of the NLS equation, where the PN barrier strictly vanishes since the model has continuous families of exact propagating soliton solutions [43].

However, as was probably first noted for a cubic model with *inter-site* nonlinearities [60], also for some non-integrable models this energy difference may vanish in particular points when parameters are varied. The considered model was derived using a coupled-mode approach to describe stationary light propagation in an optical waveguide array embedded in a nonlinear Kerr material, and after rescalings it

takes the form of an extended DNLS equation,

$$\begin{aligned} \mathrm{i}\dot{\Psi}_n = K_2(\Psi_{n-1}+\Psi_{n+1}) - \Psi_n|\Psi_n|^2 \\ +2K_4\big(2\Psi_n(|\Psi_{n-1}|^2+|\Psi_{n+1}|^2)+\Psi_n^*(\Psi_{n-1}^2+\Psi_{n+1}^2)\big) \\ +2K_5\big(2|\Psi_n|^2(\Psi_{n-1}+\Psi_{n+1})+\Psi_n^2(\Psi_{n-1}^*+\Psi_{n+1}^*)+\Psi_{n-1}|\Psi_{n-1}|^2+\Psi_{n+1}|\Psi_{n+1}|^2\big), \end{aligned} \tag{1}$$

where the time-derivative in this context should be interpreted as a spatial derivative with respect to the longitudinal coordinate. For $K_4 = K_5 = 0$, this is just the ordinary cubic DNLS model with nearest-neighbour coupling K_2 and on-site nonlinearity normalized to 1. The additional terms, whose strengths are detemined by parameters K_4 and K_5, describe two different types of nonlinear nearest-neighbour mode couplings, both resulting from the nonlinearity of the embedding medium. Like the ordinary DNLS equation, Eq. (1) has a standard Hamiltonian structure with conserved Hamiltonian (energy),

$$\begin{aligned} H = \sum_n \Big[K_2\Psi_n\Psi_{n+1}^* - \frac{1}{4}|\Psi_n|^4 + K_4\left(2|\Psi_n|^2|\Psi_{n+1}|^2+\Psi_n^2\Psi_{n+1}^{*2}\right) \\ +2K_5\Psi_n\Psi_{n+1}\left(\Psi_n^{*2}+\Psi_{n+1}^{*2}\right)\Big] + \text{c.c.} \end{aligned} \tag{2}$$

(c.c. denotes complex conjugate), as well as conserved norm (power, excitation number),

$$P = \sum_n |\Psi_n|^2. \tag{3}$$

The fundamental discrete solitons (breathers) are, just as in the standard DNLS model, spatially localized stationary solutions with a purely harmonic time-dependence,

$$\Psi_n(t) = u_n \mathrm{e}^{-\mathrm{i}\Lambda t}, \tag{4}$$

where the mode profiles u_n generically can be chosen real and time-independent.

The vanishing, at specific values of K_4, of the energy difference between on-site and inter-site solutions having the same norm is illustrated in Fig. 2, for two different values of K_5. As has been confirmed by studies of many other models (several of those to be described later in this chapter), this vanishing is generically associated with a *stability exchange* between the on-site and inter-site modes, appearing through bifurcations with a family of *intermediate*, asymmetric stationary solutions, connecting the two types of symmetric solutions and "carrying" the (in)stability between them. In fact, such a scenario for enhanced mobility had been originally described by Cretegny and Aubry [12, 2] for breathers in a KG model with a Morse potential.

One very important point to note here is, that close to such points, the *true* PN barrier (defined, as discussed in Sec. 1, as the minimum energy needed for a lattice translation of a stable soliton) is *not* equal to the energy difference between the on-site and inter-site modes, but generally *larger* since energy is needed to pass also through the intermediate stationary solution. An analogous scenario has been

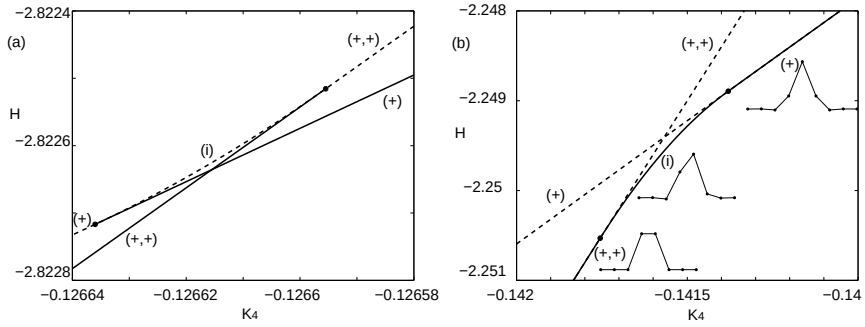


Fig. 2 Bifurcation diagrams for stationary discrete solitons in the extended DNLS equation (1) with $K_2 = 0.2$, having a constant norm (3) $P = 2$. The Hamiltonian (2) is plotted as a function of the parameter K_4 for two different values of the other inter-site nonlinearity parameter, (a) $K_5 = -0.18$, and (b) $K_5 = -0.1$. The symbols denote the three different types of solitons: on-site (+), symmetric inter-site (+,+), and asymmetric intermediate (i), with profiles (at $K_4 = -0.1416$) indicated in (b). Solid (dashed) lines denote linearly stable (unstable) solutions, and bifurcation points are indicated with dots. Figure adapted from Ref. [60].

known for a long time to appear for kinks in a modified FK model with a deformable substrate potential [63].

Another important point is to note the qualitative difference between the two scenarios in Fig. 2 (a) and (b): in (a), the intermediate solution is unstable (energy max) and the on-site and inter-site solutions are simultaneously stable in the stability exchange region, while in (b) both symmetric solutions are unstable and the intermediate solution is stable (energy min). Thus, by varying also the second parameter (here K_5), it is possible to tune the existence regime for the intermediate solution, and even to make it *vanish* at certain points! At such points, termed "transparent points" in Ref. [49] (for a different model with saturable on-site potential to be discussed below), the PN barrier is indeed truly zero and a single family of translationally invariant stationary states having the same energy and norm must exist, with a free parameter corresponding to the position of the center of energy. As elaborated for the model in Ref. [49] (see also Ref. [9] for further discussion and references), travelling waves do indeed bifurcate from stationary solutions at such exceptional points, but radiationless mobility is possible only at "special", nonzero, velocities. For generic small velocities, resonances with linear oscillations causing radiation cannot be avoided and so the mobility may be extremely good, but not perfect. An illustration of the almost perfect mobility for the model (1) very close to a transparent point was given by Öster [58] and is reproduced in Fig. 3. To our knowledge, it has not yet been investigated whether exceptional velocities with radiationless mobility exist also for Eq. (1). It was also noted in Ref. [58] that even though the Hamiltonian and norm are independent of the location of the center of energy for the family of stationary solutions at the transparent point of Eq. (1), the oscillation frequency Λ is not. It was also found earlier, for slowly moving breathers in the stability exchange regime of the KG chain with Morse potential, that the lo-

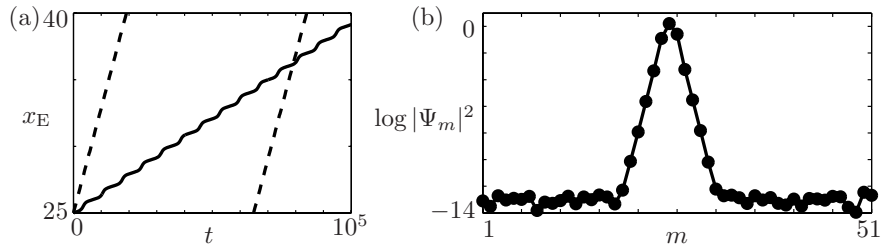


Fig. 3 Propagating excitation very close to a transparent point in the extended DNLS equation (1) with $K_2 = 0.2$, $K_4 = -0.1316$, $K_5 = -0.1470$, $P = 2.01464$, and $H = -2.61566$. (a) shows the motion of the center of energy in a 51-site lattice with periodic boundary conditions. The (unstable) on-site stationary solution is perturbed by a phase gradient e^{ikm} with $k = 10^{-4}$ (solid) and $k = 10^{-3}$ (dashed) (m here denotes site index). The non-constancy of the velocity for the very slowly moving solution (solid) is a result of the finite numerical precision when determining the transparent point; the remaining PN barrier is of the order of 10^{-7}. (b) shows a snap-shot of the slowest excitation at $t = 1000$. Note the very small but non-vanishing tail, which is larger than the numerical accuracy and thus a result of the emitted radiation during the motion. From Ref. [58].

cal oscillation frequency is not constant but varies with the location in the unit cell [12, 2].

As mentioned above, a similar scenario appears also for a DNLS model with a *saturable* nonlinearity, which can be obtained from Eq. (1) by removing the inter-site nonlinear terms ($K_4 = K_5 = 0$) and replacing the cubic on-site nonlinearity with the term $\beta\Psi_n/(1+|\Psi_n|^2)$. The Hamiltonian can then (after a trivial gauge transformation) be written as $H = \sum_n[\beta\ln(1+|\Psi_n|^2) + K_2|\Psi_{n-1} - \Psi_n|^2]$. This model is often used for describing spatial solitons in photorefractive waveguide arrays, and as was originally discussed by Hadžievski et al. in 2004 [33], there are multiple points where the energy difference between on-site and inter-site discrete solitons vanish, and a very good mobility was observed. Many works have followed discussing various properties of these modes, of which we here just mention a few. Khare et al [42] obtained analytical solutions for a complete family of intermediate solutions, Cuevas and Eilbeck [13] studied discrete soliton interactions, Melvin et al. [49] found, as mentioned above, radiationless travelling waves at "special" velocities, and Naether et al. [57] analyzed the PN potential landscape in the stability exchange regimes using a constraint method to be described in the next section. We will also return to discuss the 2D version of the saturable DNLS and its mobility properties in the next section.

3 Discrete soliton (breather) mobility in 2D

As is commonly known, mobility in 2D is "normally" much worse than in 1D, at least when the effective nonlinearity is cubic as in the standard DNLS-type models.

As discussed e.g. in Ref. [11], the reason for this can be traced to the fact that in the continuum limit, 2D NLS solitons are unstable and may undergo collapse into a singularity spike in a finite time. In a lattice, the strict mathematical collapse is impossible due to norm conservation, but instead a "quasicollapse" scenario appears where broad discrete (stationary or moving) solitons are transformed into highly localized and strongly pinned modes [11]. Moreover, it is important to note that, in contrast to the 1D case with cubic nonlinearity where the norm goes to zero in the small-amplitude (continuum) limit, the norm of 2D small-amplitude discrete solitons goes to a finite, nonzero value. The consequence is the existence of an *excitation threshold*, i.e., a minimum value of the norm below which no localized excitation exists, which has been rigorously established in Ref. [72] (see also the recent discussion in Ref. [37]).

However, some notable exceptions to the general folklore "mobility is bad in 2D lattices" has been known for some time, and we here try to briefly exemplify different physical situations where good 2D mobility of localized modes has been observed, and explain why the scenarios differ from the generic one described above.

(i) Moving breathers in vibrational lattices with several degrees of freedom, (e.g. longitudinal and transversal), such as the two-component hexagonal lattice used by Marín, Eilbeck and Russell [47] to simulate the motion of quasi-one-dimensional "quodons" along certain directions in a mica-like structure. In this case, the vibrational direction singles out a preferred direction for the breather which breaks the 2D lattice symmetry. As a consequence, along "suitable" lattice directions the breather may strongly deform and become elongated along one direction and compressed along the other. Thus it should behave essentially as a 1D small-amplitude breather in this direction.

(ii) Moving 2D polarons have been observed in electron-phonon coupled lattices with anharmonic vibrational degrees of freedom, such as the Holstein model with saturable anharmonicity in Ref. [75]. In this case, the effective nonlinearity in the semiclassical dynamics is no longer purely cubic but saturable, and as will be discussed in detail below (Sec. 3.1), such nonlinearity allows for stable, mobile localized modes also in 2D. Recently, another example of a system which may support mobile 2D polarons was given in Ref. [54], where a molecular lattice having both intra- and inter-molecular harmonic degrees of freedom was considered, and the electron-lattice coupling was assumed to have as well an on-site (Holstein) as an inter-site (Peierls) part. By tuning the relation between these two couplings suitably, mobile polarons were observed in a rather narrow parameter window. Thus, this mechanism of enhanced mobility by competing effective on-site and inter-site nonlinearities is reminiscent of the scenario for the 1D extended DNLS model (1).

(iii) Strongly anisotropic lattices, with essentially 1D mobility in the strong-coupling direction only. Typically these states are elongated, and strongly localized in the weak-coupling direction only, where they are not mobile. For anisotropic DNLS models, this scenario was described in detail in Ref. [32]. A related example is the "reduced-symmetry" gap solitons [26], where, although the lattice itself is isotropic, there is an effective anisotropy induced by anisotropic dispersion at a band edge of a higher band (e.g. *p*-band). This scenario was analyzed in detail within a

discrete coupled-mode approach in Ref. [40], where each lattice site is assumed to support two orthogonal, degenerate modes of dipolar character. With this approach, the mechanism of symmetry breaking thus becomes analogous to that of the two-component vibrational lattice discussed in (i) above, with the orientation of the local dipole corresponding to the direction of local lattice vibration in (i).

(iv) Moving, stable, small-amplitude "quasi-continuous" breathers (wide relative to the lattice spacing) were found in (scalar) 2D FPU-type lattices, square [6] as well as hexagonal [7]. Although a standard continuum approximation to lowest order yields a cubic NLS equation, where stable localized solutions do not exist as discussed above, their existence in the 2D FPU-lattice was explained by incorporating higher-order dispersive and nonlinear terms as perturbations, which under certain conditions could lead to stabilization. A similar effect was seen for moving solutions of very small amplitude in the cubic on-site DNLS equation [1]. Essentially, the velocity makes the effective dispersion of the corresponding continuum NLS model anisotropic, resulting in a deformation of broad solitons which may move for rather long distances without collapsing or trapping. However, it was noted in Ref. [1] that also these moving quasi-continuous solutions are weakly unstable and slowly decaying through dispersion in the DNLS lattice.

(v) Systems with non-cubic effective nonlinearities in the equations of motion. For a quadratic nonlinearity, there are no collapse instabilites in the continuum limit in 2D, and no excitation threshold for discrete solitons. Thus, as shown in Ref. [68] for a 2D lattice with second-harmonic generating nonlinearity, the PN barrier for small-amplitude, weakly localized solutions may be small enough for good mobility in arbitrary lattice directions. The case with saturable nonlinearity [69, 56] has already been mentioned above in (ii) and will be disussed in detail in Sec. 3.1 below. A similar mobility scenario appears also for a 2D DNLS model with competing (i.e., of different sign) cubic and quintic on-site nonlinearities [10] (resulting e.g. from taking into account only the lowest-order terms in a Taylor expansion of a full saturable potential).

(vi) Systems with flat, i.e. dispersionless, linear bands, such as the DNLS model for a Kagome lattice [70] to be described in more details in Sec. 3.2. In this case, the absence of linear dispersion implies that discrete solitons bifurcating from the flat band cannot be described by a continuous NLS equation, and therefore they are not prone to collapse instabilities. Instead, they bifurcate from localized linear modes with zero norm threshold also for cubic nonlinearities, and small-amplitude solutions can be movable while being still strongly localized due to the smallness of the PN-barrier in some regime.

3.1 Discrete soliton mobility in the 2D saturable DNLS model

The mobility properties of discrete solitons in the 2D DNLS model with a saturable on-site nonlinearity were first described in Ref. [69] and further analyzed in Ref. [56]. With the notation from Ref. [69], describing spatial solitons in a pho-

torefractive waveguide array, the dynamical equation takes the form

$$i\frac{\partial u_{n,m}}{\partial \xi} + \Delta u_{n,m} - \gamma \frac{u_{n,m}}{1+|u_{n,m}|^2} = 0, \tag{5}$$

where ξ is the normalized propagation distance along the waveguides (playing the role of the time coordinate in the standard Hamiltonian framework), $u_{n,m}$ describes the (complex) electric-field amplitude at site $\{n,m\}$, and Δ represents the 2D discrete Laplacian, $\Delta u_{n,m} \equiv u_{n+1,m} + u_{n-1,m} + u_{n,m+1} + u_{n,m-1}$, defining the linear interaction between nearest-neighbour waveguides. The two conserved quantities for Eq. (5) are the Hamiltonian (energy)

$$H = -\sum_{n,m} \left[(u_{n+1,m} + u_{n,m+1})\, u^*_{n,m} - \frac{\gamma}{2} \ln(1+|u_{n,m}|^2) + \text{c.c.} \right], \tag{6}$$

and the power (norm)

$$P = \sum_{n,m} |u_{n,m}|^2. \tag{7}$$

As illustrated in Fig. 4, there are three different types of fundamental symmetric stationary solutions, $u_{n,m}(\xi) = U_{n,m} e^{i\lambda\xi}$, which will here be termed 1-site, 2-site, and 4-site modes, respectively, referring to the number of sites sharing the main peak of the modes. (These modes go under various other names in the literature, e.g., in Ref. [37] they are termed vertex-, bond- and cell-centered bound states, respectively.) Note that there are two, degenerate, 2-site modes, horizontal and vertical. In bifurcation scenarios similar to that discussed for the 1D cases above, 1-site, 2-site and 4-site modes may exchange their stability properties under variation of the parameters γ and P, and as described in [69], mobility then appears along axial directions in certain parameter regimes. An example of the stability exchange between a 1-site and a 2-site mode, with the appearance of an unstable asymmetric intermediate solution (IS), is illustrated in the lower part of Fig. 4.

In order to better understand the conditions for mobility in the various regimes, a numerical method was implemented in Ref. [56] for calculating the full PN potential landscapes, showing the variation of the energy with the center of mass for localized solutions. The basic idea builds on the standard Newton-Raphson (NR) scheme for calculating stationary soliton solutions to the equations of motion (5) (see, e.g., Ref. [28]), but imposes two additional constraints in order to fix the center of mass of the soliton horizontally and vertically:

$$X \equiv \frac{\sum_{nm} n|u_{n,m}|^2}{P} \quad \text{and} \quad Y \equiv \frac{\sum_{nm} m|u_{n,m}|^2}{P}\,. \tag{8}$$

Technically, this is implemented by eliminating the equations for two specific sites, chosen close to, but away from, the soliton center site, from the NR iteration, and instead determining the amplitudes for these sites (which can be chosen real and positive for the fundamental solitons) from the constraint conditions (8). (See Ref. [56] for further details and discussions about optimal choices of constraint sites.) Start-

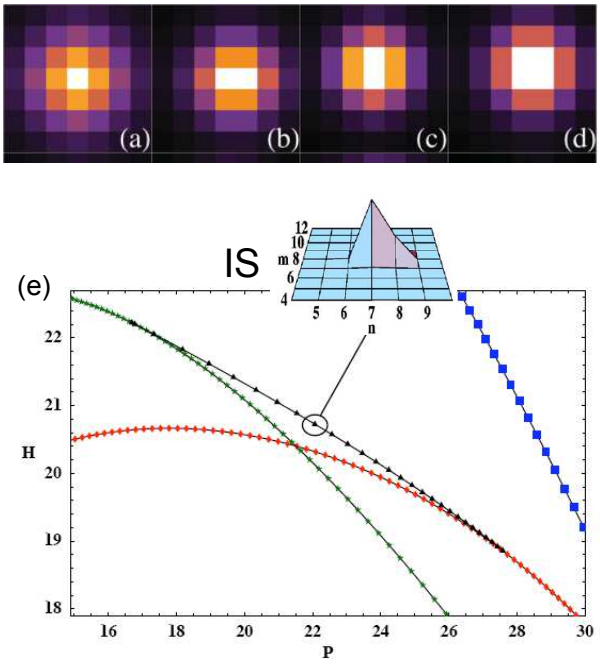


Fig. 4 Upper figures: examples of spatial profiles for the fundamental symmetric stationary solutions of the 2D saturable DNLS model (5): (a) 1-site, (b) 2-site horizontal, (c) 2-site vertical, and (d) 4-site. From Ref. [56]. Lower figure (e): Bifurcation diagram showing the exchange of stability when $\gamma = 10$ for increasing power from stable 1-site (red diamonds) to stable 2-site (green stars) via an unstable intermediate solution (IS, black triangles) with profile indicated as inset. The 4-site solution (blue squares) is unstable in this regime. Adapted from Ref. [69].

ing then from a stationary solution, e.g., a 1-site solution with center of mass at some lattice site $(X,Y) = (n_c, m_c)$, we may proceed with a numerical continuation (at fixed power P) by increasing adiabatically e.g. X in the constraint (8), until we end up at the horizontal 2-site solution centered at $(X,Y) = (n_c + 1/2, m_c)$. From there, we may continue by increasing Y adiabatically towards the 4-site solution at $(X,Y) = (n_c + 1/2, m_c + 1/2)$. Assuming that all NR iterations converge, it should be clear that the continuation could be done in any direction, and that we can also continue, e.g., with increasing Y for any X between n_c and $n_c + 1/2$.

By calculating the energy (6) for each converged, constrained solution obtained from a sweep over the full area $n_c \leq X \leq n_c + 1/2,\ m_c \leq Y \leq m_c + 1/2$, we obtain a smooth PN potential surface if the continuation is smooth everywhere. A good mobility should then be expected if there are directions where these surfaces are smooth and flat. Note that only the *local extrema* of these surfaces may correspond to true stationary solutions of the *unconstrained* system (5): stable solutions corre-

spond to minima and unstable solutions to maxima or saddles.[1] This type of method for calculating PN potentials was originally proposed for 1D breathers by Cretegny and Aubry [12, 2], and similar methods were implemented e.g. for 1D kinks in KG chains [66], and applied to surface modes in the 1D DNLS model [52].

An extensive discussion about the nature of the obtained PN surfaces in different parameter regimes, and the associated mobility properties, was given in Ref. [56]; here we just give a brief summary and show sample results for two particularly interesting regimes when $\gamma = 4$, where smooth, complete surfaces were found for all values of the power P. In the low-power regime, the surfaces have single minima corresponding to the stable 1-site modes, saddle points corresponding to the unstable 2-site modes, and maxima corresponding to the likewise unstable 4-site modes. This ordering of energies for the stationary solutions is the same as for the ordinary (cubic) DNLS model (see, e.g., Ref. [37]), which could be expected since a small-power expansion of the saturable nonlinearity yields a cubic term to lowest order. However, as discussed above, for the cubic 2D DNLS model, stable stationary solutions are not mobile due to the large power excitation thresholds and narrowness of the stable solutions. The effect of the saturability is to lower the excitation thresholds for all three stationary solutions [69], allowing for the existence of a regime of relatively low power with broader stable modes having improved mobility [69, 56]. In terms of PN potentials, this results in smooth, complete 2D surfaces generated from the constrained NR method, which could not be obtained for the cubic DNLS model [56].

For increasing power, the scenario changes as the first stability exchange regime (illustrated in Fig. 4 for a different value of γ) is reached. In Fig. 5, two new saddle points corresponding to the unstable, asymmetric, stationary intermediate solutions (IS) have appeared, while the extrema corresponding to the (now stable) 2-site modes have changed to local minima. Note that the energy landscape is almost flat between the simultaneously stable 1-site and 2-site solutions, resulting in a very good axial mobility (lower plot in Fig. 5). Note also how the very slowly moving mode in Fig. 5 clearly traces out the local features of the PN potential in the axial directions, where the velocity is minimal at each location for the center of mass corresponding to IS saddles in the potential surface.

A further increase in P turns the 1-site mode unstable, and the PN surface for the regime when only the 2-site modes are stable is shown in Fig. 6. Note that the topology of the surface, with two equivalent minima corresponding to the stable horizontal and vertical modes and two local maxima corresponding to the unstable 1-site and 4-site modes, necessitates a saddle point along the diagonal between the maxima, and therefore another asymmetric unstable stationary intermediate solution (here termed IS2) must exist. The flatness of the energy landscape (note the scale on the H-axis) between the stable horizontal and vertical 2-site modes implies a new type of mobility in the diagonal direction, illustrated in the lower part of Fig. 6:

[1] A cautionary remark may be in order: if the constraint sites are not properly chosen, the method may reach different stationary solutions, or no stationary solutions at all [56], and therefore yield different energy landscapes not related to the PN potential between the fundamental 1-site, 2-site and 4-site modes.

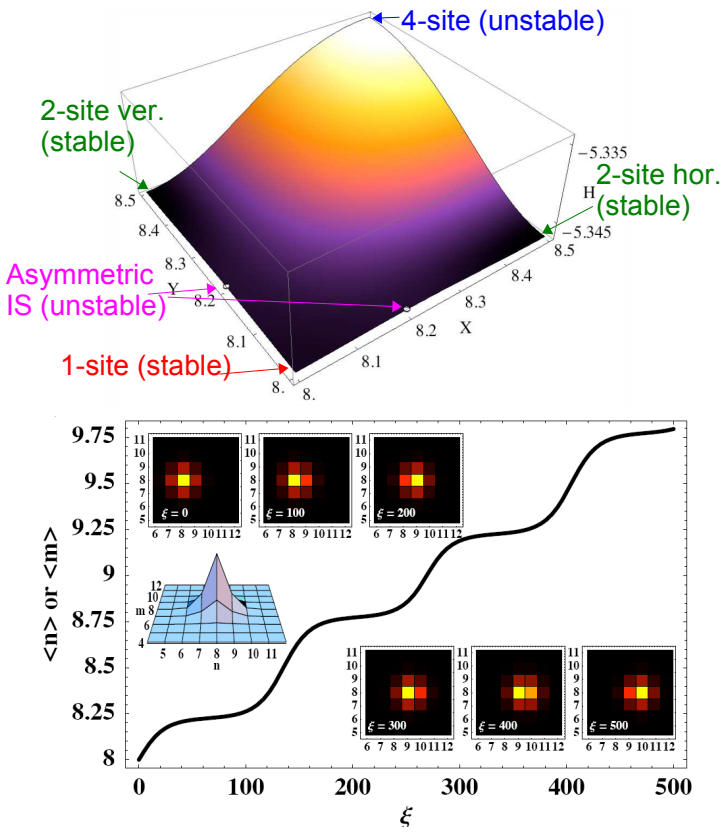


Fig. 5 Upper figure: PN potential surface of Eq. (5) for $\gamma = 4$ and $P \approx 9.4$. The different stationary solutions are marked with arrows. Adapted from Ref. [56]. Lower figure: The resulting mobility in an axial direction, after applying a small phase gradient ($k \approx 6 \cdot 10^{-3}$) to a stable 1-site mode, which adds an energy just enough to overcome the very small PN barrier ($\Delta H \approx 2 \cdot 10^{-4}$) to the stationary intermediate solution (IS). Main figure shows motion of center of mass, inset shows profiles at different ξ. From Ref. [69].

the soliton moves its center along the diagonal by repeatedly transforming between horizontal and vertical shapes, passing over the small PN barrier created by the intermediate solution (see Ref. [56] for further illustrations).

Continuing the increase of power, a fourth regime is reached where also the 4-site solution has stabilized (this occurs when the IS2 saddle in Fig. 6 reaches the 4-site max), yielding a PN surface with local minima at the stable 2-site and 4-site positions, a maximum at the unstable 1-site position, and saddles corresponding to new unstable intermediate solutions between 2-site and 4-site modes [56]. The energy landscape is now almost flat between the 2-site and 4-site positions, resulting

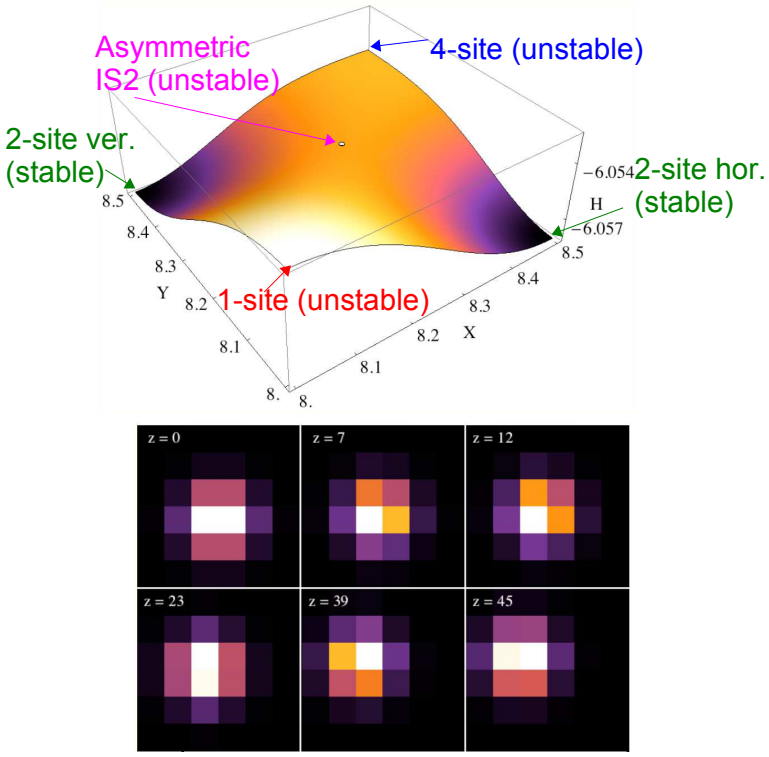


Fig. 6 Upper figure: PN potential surface of Eq. (5) for $\gamma = 4$ and $P = 10.0$, with stationary solutions marked with arrows. Lower figure: The resulting mobility in a diagonal direction, after applying a small phase gradient ($|k_x| = |k_y| = 0.018$) to a stable horizontal 2-site mode (here, z is used instead of ξ to denote the time-like variable in Eq. (5)). Adapted from Ref. [56].

again in a very good mobility along axial directions but now between the 2-site and 4-site modes [56].

Finally, a fifth qualitatively different regime is reached when increasing P, where the 2-site solutions have turned unstable and only the 4-site mode is stable [69, 56]. Thus, the PN surface has only one minimum at the 4-site position, saddles at the 2-site positions and maximum at the 1-site position. There are no intermediate solutions but, as illustrated in Ref. [56], the PN potential may still be sufficiently smooth and flat to allow for mobility in, e.g., diagonal directions with an appropriate initial perturbation.

A further increase in power yields repeated stability exchanges [69, 56], and so the above described five different regimes of qualitatively different PN potentials, and their corresponding characteristic mobility properties, will reappear repeatedly [56]. Among other issues discussed in Ref. [56], it was also shown that including weak lattice anisotropy breaks the symmetry between the horizontal and vertical 2-site modes, thereby allowing for two additional PN surface topologies (see

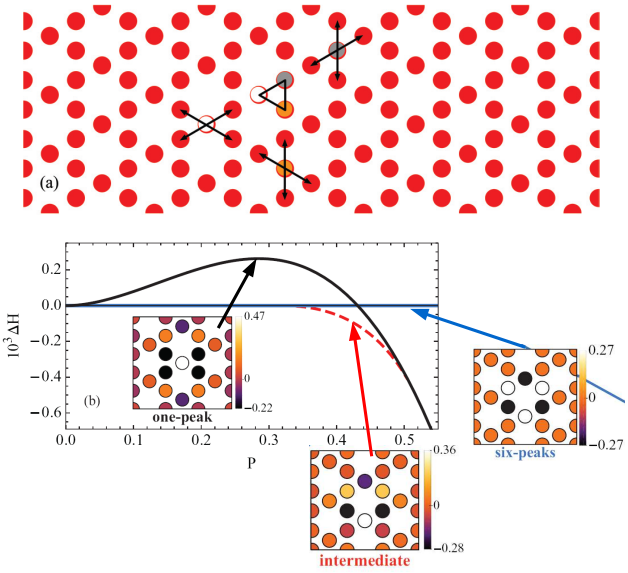


Fig. 7 Upper figure: Structure of the Kagome lattice showing a unit cell with three sites (triangle) and the directions of their respective nearest-neighbour interactions. Lower figure: Hamiltonian (relative to the six-peaks solution) versus power for the fundamental stationary nonlinear localized modes of Eq. (9) with amplitude profiles (for $P = 0.43$) as indicated. Adapted from Ref. [70].

Ref. [56] for details). In particular, it was seen that for a non-negligible anisotropy, all intermediate solutions appear on the edges of the surfaces (i.e., scenarios with IS2-type solutions as in Fig. 6 disappear), implying that the best mobility for anisotropic lattices should generally appear along lattice directions. Thus, in conclusion, calculating the full 2D PN potentials appears as a very powerful tool for predicting the directional mobility properties in 2D lattices.

3.2 The Kagome lattice

In this subsection, we summarize and discuss results obtained in Ref. [70] (to which the reader is referred for further details and references) regarding the mobility properties of the so called "discrete flat-band solitons" in the 2D Kagome lattice. The structure of the Kagome lattice is illustrated in Fig. 7, and as indicated in the figure, it can be viewed as a hexagonal lattice with a three-site, triangular unit cell. We will consider the ordinary, cubic, on-site DNLS model defined with nearest-neighbour interactions according to the Kagome lattice structure as indicated in Fig. 7, which with the notation of Ref. [70] takes the form

$$i\frac{\partial u_{\mathbf{n}}}{\partial z}+\sum_{\mathbf{m}}V_{\mathbf{n},\mathbf{m}}u_{\mathbf{m}}+\gamma|u_{\mathbf{n}}|^2u_{\mathbf{n}}=0\ , \tag{9}$$

where z corresponds to the time-like variable, $u_{\mathbf{n}}$ represents the field amplitude at site $\mathbf{n}$, and the sum over $\mathbf{m}$ is restricted to nearest neighbours to $\mathbf{n}$ in the Kagome lattice. Here, it is crucial to note that we consider exclusively the case with defocusing nonlinearity, which implies that with a proper normalization we can put $\gamma=-V_{\mathbf{n},\mathbf{m}}\equiv-1$.

The linear spectrum ($\gamma=0$) of Eq. (9) is well known (see, e.g., Ref. [3]): of its three (connected) bands, the lowest one is exactly flat (dispersionless). As shown in Ref. [3], the flat band contains as many states as the number of closed rings in the lattice, and thus can be considered to be built up from "six-peaks" (or "ring") solutions, where six sites in a closed hexagonal loop have equal amplitude but alternating phases, with exactly zero background. (The zero background results from the frustration property of the Kagome lattice: each site immediately outside a ring mode couples identically to two sites in the ring, but since these sites have opposite phases, their contributions cancel out due to destructive interference.) The amplitude profile of a six-peaks mode is show in the lower, rightmost part of Fig. 7.

For a defocusing nonlinearity ($\gamma<0$), nonlinear stationary solutions to Eq. (9) will bifurcate from the lowest-energy linear band, i.e., the flat band [70]. It is easily seen, that the single six-peak ring mode is an exact (and strictly compact!) stationary solution also in the nonlinear case, and that it exists for all possible values of power, $0\leq P<\infty$. Consequently, in sharp contrast to the case for ordinary 2D DNLS lattices (having dispersive bands) with cubic nonlinearity discussed in the beginning of this section, there is no power (norm) threshold for creation of localized stationary solutions in the flat-band Kagome lattice.

Moreover, also other nonlinear stationary solutions bifurcate from linear combinations of the degenerate fundamental linear flat-band ring modes, and the nonlinearity will generally break the degeneracy of such solutions. In contrast to the single-ring, six-peak, solution, these nonlinear solutions will generally not remain compact but develop an exponential tail [70], as for "ordinary" lattice solitons/breathers. Of special interest is the mode obtained by adding together two neigbouring ring modes having one site in common, which thus in the linear limit gets an amplitude twice as large as the other ten sites in the rings. Also this solution belongs to a family of nonlinear localized stationary solutions existing for all values of power [70], and in the limit $P\to\infty$ ("anticontinuous limit"), it becomes a single-site localized excitation. The profile of this solution, here termed "one-peak", is illustrated for a small but nonzero power in the lower left part of Fig. 7 (note that the two contributing rings are vertically aligned in this figure).

Comparing the Hamiltonian (energy) at fixed power (norm) for these two families of solutions, it can be checked [70] that the single-ring (six-peaks) mode has the lowest energy and constitutes the ground state of the system close to the linear limit, while the double-ring (one-peak) mode is the ground state for strong nonlinearity. Thus, as illustrated in the lower part of Fig. 7, there is an exchange of stability between these two modes, with a scenario similar to what has been described for other

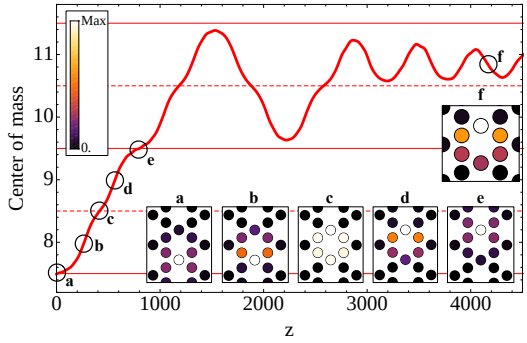


Fig. 8 Main figure: Evolution of the vertical center of mass when applying a very small vertical kick ($k_y = 0.009$) to an unstable one-peak solution in the stability-exchange regime of Fig. 7 ($P = 0.4655$). Horizontal lines mark out the locations of stationary one-peak (solid) and six-peaks (dashed) modes. Insets show intensity profiles $|u_{\mathbf{n}}(z)|^2$ of the travelling mode at the indicated locations (a)-(f). From Ref. [70].

models above, with appearance of an asymmetric, intermediate stationary solution in the exchange regime. In fact, the scenario is here analogous to that of Fig. 2 (b), with simultaneous instability of the on-site (one-peak) and inter-site (six-peaks) modes and a stable, symmetry-broken intermediate solution constituting the ground state of the system.

Thus, having all previously discussed examples of connections between stability exchange and enhanced mobility in mind, it might not be unexpected that good mobility between these strongly localized, fundamental modes may appear also here,[2] and at a relatively small power as can be seen from Fig. 7. The results from applying a small vertical kick (phase gradient) on an unstable one-peak mode in the stability-exchange regime is show in Fig. 8. As can be seen, the initial movement is quite analogous to previously discussed cases (cf., e.g., Fig. 5) and nicely traces out the features of the PN potential in the corresponding direction, with smallest velocities in the unstable one-peak ((a), ((e)) and six-peaks ((c)) positions, and largest velocities in the stable intermediate positions ((b), (d)). For the very tiny kick in Fig. 8, the mode quickly loses its surplus energy due to radiation effects, and finally gets trapped with small oscillations around an intermediate stationary solution ((f)), constituting its symmetry-broken ground state in this regime. As discussed further in Ref. [70], the distance travelled in the lattice may be controlled to some extent by the kick strength, thus yielding a mechanism for controlled transfer, in particular directions of the Kagome lattice, of small-power strongly localized modes in a 2D DNLS-lattice with standard (cubic) nonlinearity.

We end this subsection with a brief mentioning of some earlier works discussing nonlinear localized modes in Kagome lattices. Law et al. [45] also considered the

[2] The reader should however be cautioned that there are counter-examples where mere stability exchange does *not* imply good mobility, as for the 2D version of Eq. (1) [59], since it does not automatically imply that a smooth and flat PN surface exists in the full domain.

defocusing case, but concentrated on vortices and complex structures mainly in the strong-nonlinearity regime, without making connections to flat-band linear modes or mobility. Zhu et al. [74] studied defect solitons with saturable nonlinearity, and Molina [51] localized modes in nonlinear photonic nanoribbons; however, both these works considered the case of focusing nonlinearity, which follows the standard 2D NLS phenomenology with threshold etc., since the upper band is non-degenerate [3, 70].

4 Travelling discrete dissipative solitons with intrinsic gain

The discussion in the previous sections has dealt exclusively with conservative lattices (i.e., conserved energy), and in addition we have seen that the analysis of breather mobility in terms of PN potentials needs a second quantity to be (at least approximately) conserved (typically action, or norm/power for DNLS-type models). As we also discussed, unless we succeed to tune our model parameters into an exact "transparent point", and succeed to give our breather a "special" velocity (or succeed to find some other exceptional system like an integrable model), moving breathers in Hamiltonian lattices are not exponentially localized outside their main core, but develop an extended tail due to radiation even when the PN potentials are very smooth and flat. The tails may be very weak (as e.g. the example shown in Fig. 3 (b)), but due to the radiation continuously emitted, a breather travelling in a large lattice will typically in the end get trapped around some minumum of the PN potential.

In a dissipative environment, the situation will naturally be quite different. Pure losses will evidently damp out the radiative tails, but also the energy of the breather core. However, if there is some additional intrinsic gain mechanism (such as for a lasing system in optics), one could hope to, under certain conditions, establish a balance (at least when averaged over time) where the gain is strong enough to support a (possibly strongly localized) moving breather indefinitely, but weak enough not to destroy the exponentially decaying tail. That this indeed is possible, under certain conditions, was demonstrated recently in Ref. [39] for a model of a 1D waveguide array in an active Kerr medium with intrinsic, saturable gain and damping. Here we will briefly summarize and discuss some of the main results from Ref. [39], to which we refer for details and further references.

Under the assumption of a pure on-site Kerr nonlinearity, the model studied in Ref. [39] (originally suggested by Rozanov's group, see Ref. [44] and references therein) is a generalized Discrete Ginzburg-Landau (DGL) type model which can be written in the form

$$i\dot{\psi}_n + C(\psi_{n-1} + \psi_{n+1}) + \left(V_n + |\psi_n|^2 - i f_d(|\psi_n|^2)\right)\psi_n = 0. \tag{10}$$

Thus, Eq. (10) is equivalent to the pure on-site version of Eq. (1) (we will comment briefly below also on the extension to intersite nonlinearities, $K_4 = K_5 \neq 0$,

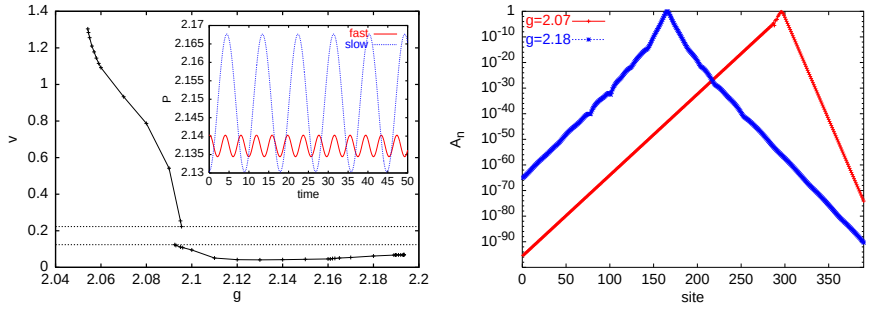


Fig. 9 Left figure: Velocity v versus gain parameter g for moving localized solutions of Eq. (10) with $V_n \equiv 0$, $C = 1$, and parameters in Eq. (11) chosen as $\delta = 1$, $a = 2$, $b = 10$. Horizontal lines indicate a gap of "forbidden" velocities, and inset shows norm oscillations for two bistable solutions at $g = 2.095$: a fast solution with small oscillations and a slow solution with large oscillations. Right figure: Snap shops of intensity $A_n = |\psi_n|^2$ for two right-moving solutions with $g = 2.07$ (right peak, fast mode) and $g = 2.18$ (left peak, slow mode). From Ref. [39].

which was discussed in some detail in Ref. [39]), with the addition of a possible linear (real) on-site potential V_n ($V_n \equiv 0$ for periodic lattice), and, most importantly, a (real) function $f_d(|\psi_n|^2)$ describing the amplification and absorption characteristics of each waveguide. [3] As in Ref. [44] (and references therein), the function $f_d(x)$ is chosen to include linear and saturable absorption, as well as saturable gain, and can after proper normalizations be taken on the four-parameter form

$$f_d(x) = -\delta + \frac{g}{1+x} - \frac{a}{1+bx}, \quad \delta, g, a, b > 0. \tag{11}$$

The parameters describe, respectively, linear losses (δ), saturable gain strength (g), saturable absorption strength (a), and ratio between gain and absorption saturation intensities (b). As detailed in Refs. [44, 39], the conditions to have localized modes which simultaneously should have a stable zero-amplitude tail, and a core with a non-zero, non-decaying amplitude, put several restrictions on the possible parameter intervals (it also follows that $b > 1$, i.e., the gain must saturate at a higher intensity than the damping). The observant reader will notice that expanding Eq. (11) to second order in x yields a cubic-quintic DGL model, which may be a more familiar system (see, e.g., Ref. [19]). However, as was found empirically by extensive numerical searches in Ref. [39], the relevant solutions describing moving localized modes essentially result from the strong saturabilities of the gain and damping parts on different intensity scales, and therefore in regimes not well described by a cubic-quintic approximation.

In Fig. 9 we illustrate a typical scenario with moving, strongly localized solutions for a "suitable" regime of parameter values (see Ref. [39] for further discussions

[3] For simplicity, C is chosen real, i.e., absorption or gain in the medium between the waveguides is neglected.

on the influence of parameter variations). As can be seen, gain-driven, travelling discrete solitons exist as exact exponentially localized solutions at specific velocities, although in a rather narrow interval for the gain parameter. It is important to note that, in contrast to conservative systems where there are continuous families of breathers/solitons as discussed above (which can be parametrized e.g. using the norm/action, or frequency, as parameter), breathers/solitons in dissipative systems generically appear as isolated attractors where an appropriate balance between energy input and dissipation can be established (see, e.g., Refs. [28, 29] and references therein). Here, for most values of g where moving solitons are found as attractors, they have a well-defined, single velocity v, which typically increases for smaller gain (although the dependence generally is not strictly monotonous as seen in Fig. 9, left part). Note also the division in a "fast" and a "slow" branch, with a forbidden velocity gap and a small regime of bistability.

The exponential localization of the moving solitons is illustrated in the right part of Fig. 9. Two features are noteworthy: (i) a crossover between one decay rate around the soliton core, and another (generally weaker) in the tails; (ii) the stronger decay rate in the forward than in the backward direction (particularly visible for the fast soliton). As discussed in Ref. [48], the latter is an effect of the radiation emitted from the breather core during its motion being Doppler shifted.

As can be seen from the inset in the left figure in Fig. 9, the norm (power) of the moving solutions is not constant but oscillates time-periodically during the motion; similar oscillations (with the same period) occur for the Hamiltonian (energy) [39]). The necessity for such oscillations in order to sustain an exact moving, strongly localized discrete soliton has a simple, intuitive interpretation in terms of the PN potential of the corresponding conservative system: in order to overcome the PN barrier and travel with a constant average velocity, the soliton may adjust its internal degrees of freedom to its lattice position by locally absorbing and emitting "suitable" amounts of norm and Hamiltonian via the gain and damping terms, respectively. As seen in Fig. 9, the largest oscillations typically appear for the "slow" solitons appearing for the larger gain values; essentially these solitons also have a higher peak power and are more strongly localized, and therefore the corresponding effective PN potential should be stronger.

In the main part of the regime where moving solitons exist, the oscillations in P and H are 1:1-locked with the soliton translation, i.e., the soliton returns to its initial shape after translation with one site. However, as discussed in more detail in Ref. [39], when approaching the rightmost part of the existence regime for g in Fig. 9, the soliton undergoes a sequence of period-doublings (i.e., the soliton does not return to its initial shape until after a translation with 2^k sites), until it loses its regular movement and enters a regime of apparently random motion. For other parameter values, also small windows of period-3 translational motion were found in Ref. [39].

As mentioned above, the existence regime for moving discrete solitons in the model (10) is quite narrow, which can be related to the non-negligible PN barrier for strongly localized modes of the ordinary (conservative) cubic DNLS model. However, as was discussed in Sec. 2, inter-site nonlinearities as in Eq. (1) may drastically

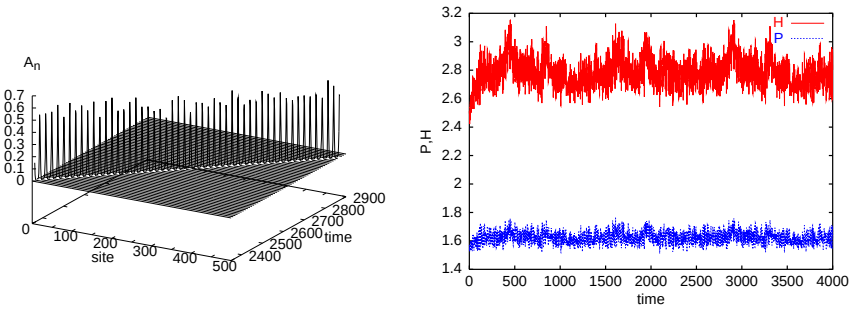


Fig. 10 Left figure: Intensity distribution for soliton moving with constant velocity $v \approx 0.977$ in a lattice with a uniformly distributed, disordered on-site potential $V_n \in [-0.1, 0.1]$. $g = 2.06$, other parameters same as in Fig. 9. Right figure: The corresponding oscillations for the Hamiltonian (upper) and norm (lower). From Ref. [39].

decrease the PN potential and improve the mobility. One may therefore suspect that, similarly, inclusion of inter-site nonlinearities also may increase the existence regime for moving solitons in the gain-damped DGL model. Without going into details (see Ref. [39]), the answer is strongly in the affirmative. For example, for the same parameter values as in Fig. 9, the existence regime in g is about five times larger when $K_4 = K_5 = -0.2$. Another effect of the weakened PN barrier is, that the internal oscillation of the soliton may become decoupled from its translational motion, resulting in a quasiperiodically moving soliton which, although it moves with constant velocity, never exactly returns to its initial shape in the lattice [39]. Also tiny regimes of non-trivial phase locking (e.g., makes two internal oscillations while moving five sites) were observed in Ref. [39].

As a final illustration of the ability of the moving discrete dissipative solitons to keep moving with constant velocity by adjusting to their local environment in the lattice, we show in Fig. 10 an example from Ref. [39] of a moving soliton in a weakly *disordered* lattice (again with pure on-site nonlinearity, $K_4 = K_5 = 0$). Although the on-site potential V_n is chosen randomly from a uniform distribution, the soliton moves indefinitely (here in a lattice with 2405 sites and periodic boundary conditions [39]) with constant velocity! It does so by, at each point, adjusting its internal parameters according to its local environment. As illustrated in the right part of Fig. 10, this results in irregular oscillations of norm and Hamiltonian, compensating for the irregularities in the lattice. A careful look at these curves confirms this scenario: although they may look random, in fact they are not. After an initial transient, they periodically repeat themselves *exactly* with a period of 2462 time units, corresponding to one round trip in the lattice!

Let us end this section with some brief discussion about other related works (a more extensive discussion was given in Ref. [39]). Surely this is not the first observation of moving discrete dissipative solitons/breathers; see, e.g., the reviews [28, 29]. Indeed, many aspects of the mobility scenarios described here are analogous to what has been reported earlier for other systems: The existence of two types of “fast” and

"slow" breathers with exponentially decaying phonon tails were described for the damped-driven FK model in Ref. [48], similar modes have been discussed in the context of "discrete cavity solitons" in optics (see, e.g., Refs. [18, 73, 17]), and also experimentally moving localized modes with similar properties have been observed in damped-driven electrical lattices [23, 24, 25]. However, conceptually, all these systems are different from the model discussed here and in Ref. [39], in the sense that they require an explicit, uniform *external* driving to supply the necessary energy to compensate for the damping. As a consequence, the moving breathers in these systems are not strictly localized but decay (exponentially) towards a tail of constant, non-zero amplitude, implying that their energy would increase towards infinity for increasing system size. By contrast, in Eq. (10) the gain results from purely *intrinsic* properies of the medium where the soliton propagates (such as, e.g., a lasing system), allowing for propagating finite-energy solitons with tails decaying towards zero.

We considered here only one particular model of a gain/damped system (admittedly, rather special with many different ingredients). It would of course be highly interesting to investigate whether travelling localized modes, driven by some intrinsic gain mechanism, can exist also in more general physical lattice systems. One particularly interesting issue, pointed out to us by Mike Russell, is the suggestion that the quodons in mica-like systems could travel for macroscopic distances thanks to an intrinsic gain mechanism, resulting from the lattice being in a metastable configuration [65].

5 Mobility of quantum lattice compactons

So far, we only discussed mobility of nonlinear lattice excitations using the language of classical physics. However, in many applications of the discrete breather/soliton concept, quantum mechanical effects may be important, and therefore it is highly relevant to investigate to what extent the above described scenarios for mobility survive under quantum fluctuations. The literature on "quantum discrete breathers" is huge and we do not make any attempt to give a complete review of this topic here, but refer the reader to Refs. [28] and [64] for discussions and further references. Let us just recapitulate some basic facts. Quantum mechanics, in the language of a many-body Schrödinger equation, is linear, and for a periodic lattice the Hamiltonian is invariant under lattice translations. Thus, all eigenstates must obey the Bloch theorem, meaning that they are necessarily delocalized and the probability of finding a particular number of excitation quanta ("particles") at a certain site must be the same at *any* site. However, it is possible to define localization in another sense, looking instead at *correlations*. Following Eilbeck [21], a quantum analogue of a classical localized breather may then be defined as an eigenstate with a high probability of having *many* quanta localized on the *same* site (or, more generally, identified as many-particle bound states with correlation functions exponentially decaying in space [71]).

Alternatively, if we insist on creating a quantum state which, like a classical soliton/breather, is localized at some *specific* site(s), we need to take an appropriate superposition of eigenstates. As discussed in Refs. [28, 64, 21] (and references therein), it is expected that when a classical nonlinear Hamiltonian lattice possesses exact discrete breathers/solitons, its quantum counterpart contains nearly degenerate bands of eigenstates, corresponding to specific many-particle bound states with different crystal momenta ("breather bands"). The bandwith of such a band is then proportional to the inverse of a "tunneling time", describing the time it takes for a semiclassical breather to perform a quantum tunneling from one site to the next. The tunneling time should become infinite in the classical limit. Note that this quantum breather tunneling is a purely quantum effect of a very different nature than the coherent mobility of a classical breather. Even though, if the breather band is well isolated from other bands, a localized excitation created from a superposition of its eigenstates will remain localized in terms of correlations (probability to find many particles at the same site remains large), it will spread symmetrically in the lattice in terms of the expectation value of the local excitation number operator. See e.g. Ref. [27] for explicit illustrations of this scenario.

Although quite much effort has been spent on understanding various properties of quantum discrete breathers [28, 64], to the best of our knowledge very little has been known about the quantum counterparts to the classically *moving* breathers, and in particular whether the concepts of PN potential and barrier have any relevance when quantum effects become strong. Clearly, a necessary condition for these concepts to make sense must be that the breather band is sufficiently narrow for the quantum tunneling time to be much larger than the inverse classical velocity (i.e., the time it takes for the classical breather to move one lattice site); otherwise, the probability distribution for the quantum breather will spread through tunneling before its center has had the time to perform a translation in a given direction. Thus, the approach of tracing out a PN potential by imagining an infinitely slow breather movement makes sense only in the classical limit.

In Ref. [36] we addressed some of these issues in the context of a 1D *extended Bose-Hubbard* (eBH) model, which is a quantum version of the classical extended DNLS model (1), for which the quantum Hamiltonian can be written in the form [35, 36]

$$\hat{H}_{eBH} = \sum_{i=1}^{f} \left\{ \frac{1}{2} Q_1 \hat{N}_i + Q_2 \hat{a}_{i+1}^\dagger \hat{a}_i + \frac{1}{2} Q_3 \hat{N}_i^2 + Q_4 \left[2\hat{N}_i \hat{N}_{i+1} + (\hat{a}_{i+1}^\dagger)^2 (\hat{a}_i)^2 \right] \right.$$
$$\left. + 2Q_5 \left[(\hat{a}_i^\dagger)^2 + (\hat{a}_{i+1}^\dagger)^2 \right] \hat{a}_i \hat{a}_{i+1} \right\} + \text{H.c.}. \quad (12)$$

Here f is the number of sites, $\hat{a}_i^\dagger (\hat{a}_i)$ is the bosonic creation (annihilation) operator, and $\hat{N}_i = \hat{a}_i^\dagger \hat{a}_i$ the corresponding number operator for particles at site i (H.c. is Hermitian conjugate). The total number of particles N is conserved since the total number operator $\hat{N} = \sum_i \hat{N}_i$ commutes with $\hat{H}_{eBH}$. This model appears e.g. in the study of ultracold bosonic atoms in optical lattices; see the very recent review [16] for extensive discussions and further references (a shorter introduction with some additional

references was also given recently in Ref. [34]). When $Q_4 = Q_5 = 0$, this is just the ordinary (on-site) Bose-Hubbard model, which is a standard model for cold atoms in optical lattices [16] and also widely studied in the field of quantum breathers since it is the quantum counterpart of the ordinary DNLS model [28, 64, 21]. Physically, Q_2 represents single-particle tunneling between neighboring sites and Q_3 a local (on-site) two-body interaction (Q_1 defines the single-particle energy scale). Also the additional nearest-neighbour interaction terms have simple physical interpretations: the first Q_4-term describes a density-density interaction between neighboring sites, the second a coherent tunneling of a particle pair, while the Q_5-terms describe density-dependent tunnelings since they depend on the number of particles at the site the particle is tunneling to and from, respectively [16]. Taking the classical limit, $N \to \infty$, in an appropriate way [36] results in the Hamiltonian (2) for a normalized classical field Ψ_i with $P = 1$ and $|\Psi_i|^2 = < \hat{N}_i > /N$, after a gauge transformation removing Q_1, a rescaling putting $Q_3 = -1/2N$, and parameter identifications $K_2 = Q_2$, $K_4 = Q_4/N$ and $K_5 = Q_5/N$.

As is well known [21, 28, 64], computational limitations are generally putting severe restrictions on the abilities to study quantum properties of classical discrete breathers with exact diagonalization, and this is most certainly so also concerning mobility issues. Ideally, we would like to study systems with many particles to get in contact with the classical world, and large lattices to observe localization and translation over some distances. However, the dimension of the matrices obtained from Eq. (12) for a given N grows as $(N+f-1)!/N!(f-1)!$, so if we wish to study large lattices we are restricted to very few particles, and if we wish to study many particles we are restricted to very few sites! Here, we may use the latter approach due to a special property for discrete soliton solutions of the classical model (1): as was found in Ref. [60], at specific parameter values the solitons become strictly *compact*, i.e., completely localized at a small (in fact, arbitrary) number of sites with exact zero amplitude outside. Of particular interest here is the symmetric intersite breather denoted (+,+) in Fig. 2, which compactifies into a two-site compacton when $K_5 = -K_2/P$, where the effective tunneling to outside neighboring sites vanishes. In fact, this is precisely the case illustrated in Fig. 2(b) as also indicated by the (+,+) profile in the inset. Thus, for some interval in K_4 close to the bifurcation points, extremely narrow mobile classical solutions exist as was also confirmed by direct numerical integrations in Refs. [60] and [36] (if $K_5 = -K_2/P$ exactly, the core of the moving classical state will have a rapidly decreasing exponential tail which compactifies each time it passes an intersite configuration; if the condition is not exactly fulfilled its core always decays exponentially but very rapidly as illustrated in Fig. 3(b)).

Thus, by focusing on quantum counterparts to the compact classical modes, we may restrict our studies to very small lattices in order to investigate their mobility; here we discuss results obtained in Ref. [36] for $f = 4$ and periodic boundary conditions. For the quantum model (12), it can be shown that only one-site classical compactons have counterparts which are exactly compact also as quantum eigenstates [35, 36]. However, the one-site compactons are less interesting in the present context since they are not classically mobile. The two-site compactons

correspond instead to quantum states with a small, and in the classical limit vanishing, probability of finding particles spread out over more than two sites [35]. In the neighbourhood of a classical stability exchange region as in Fig. 2 (b), the mobile two-site compacton also becomes the ground state when K_4 is decreased. Thus, well localized quantum states may be constructed by taking properly chosen [36] linear combinations of eigenstates in the lowest-energy band. If left untouched, these states will spread through tunneling with a tunneling time increasing with N as discussed above. Far from the classical stability exchange regime, where the ground-state band is narrow and well isolated from other bands, the tunneling times are large and grow rapidly (exponentially) with N; however, approaching the classical stability exchange several bands will interact and/or cross, resulting in tunneling times becoming much shorter and only slowly increasing with N [36]. An analogous rapid spreading resulting from hybridization of bands having their main particle occupation on a single site and on two sites, respectively, was also briefly mentioned in Ref. [15] for a few-particle Bose-Hubbard system extended with three-particle on-site repulsion (corresponding in the classical limit to a cubic-quintic on-site DNLS equation with competing nonlinearities), and was described in more detail in Ref. [27] for another extended Bose-Hubbard model, with on-site and pure density-density interactions between neighbouring sites (i.e., keeping only the first of the Q_4-terms in Eq. (12)).

In Fig. 11 we illustrate, for a system of $N = 20$ particles, the quantum dynamics of Eq. (12) resulting from using such linear combinations of lowest-energy eigenstates as initial states, after applying an initial "kick" in order to induce a directed mobility of these states. Analogously to kicking a classical soliton/breather, a phase gradient is imprinted by acting on the state with the phase operator $\exp(\mathrm{i}\theta \sum_j j\hat{N}_j)$, which corresponds to imposing a classical phase gradient θ as discussed, e.g., in Ref. [50]. Figures (a)-(d) illustrate a typical scenario in a regime where the classical ground state is a two-site compacton. Away from the immediate neighbourhood of the stability exchange regime ((a) and (c)), we can clearly identify signs of the classical PN barrier in the quantum dynamics: in (a), when the kick is too small to overcome the PN barrier, the site population expectation values exhibit small oscillations around their initial equal distribution, slowly decaying due to the quantum tunneling, while in (c), when the kick of the same initial state is strong enough for overcoming the barrier, the main population starts to move around the lattice. On the other hand, for parameter values close to the classical stability exchange region ((b) and (d)) where the classical compacton becomes mobile already for very small kicks, the quantum tunneling times decrease as discussed above, and therefore, for small kicks as in (b), the quantum spreading takes over before the soliton has had the time to translate even one site. However, for larger kicks (d), the time scale of the classical movement becomes short enough to separate from the quantum time scale, and therefore the soliton population may move in a classical-like way for rather long distances.

Thus, the existence of a classical stability exchange regime can be said to play a "double game" for the quantum mobility of localized initial states. On one hand, it lowers the PN barrier making the movement of highly localized states at all possible.

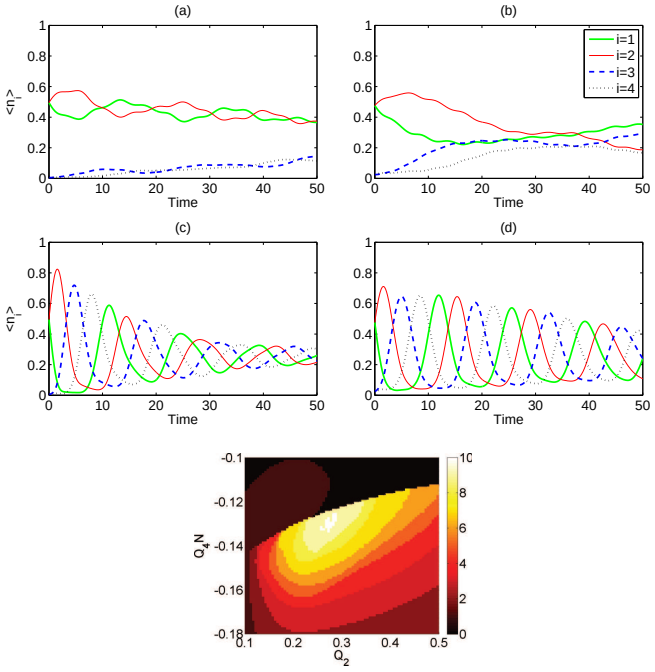


Fig. 11 Upper and middle figures: Time evolution of the expectation values of the local relative particle number operators, $< \hat{n}_i > \equiv < \hat{N}_i > /N$, for localized initial quantum states obtained from superpositions of eigenstates in the lowest-energy band of the $f = 4$-site lattice (periodic boundary conditions), after imprinting a phase gradient $\theta = 0.1$ (upper figures) and $\theta = 1$ (middle figures). The number of particles is $N = 20$. Parameter values in the eBH Hamiltonian (12) are $Q_2 = -Q_5 N = 0.3$, and $Q_4 N = -0.16$ (left figures) and $Q_4 N = -0.12$ (right figures), respectively. Lower figure: The number of sites a state with $\theta = 1$ can travel before the maximum local population expectation values have decayed to 0.4 at times when they are equal, $< \hat{n}_i > = < \hat{n}_{i+1} >$ (i.e., intersection points in (d)), plotted as functions of Q_2 and $Q_4 N$ while keeping $Q_5 N = -Q_2$ corresponding to the classical 2-site compacton condition. $f = 4, N = 20$. Adapted from Ref. [36].

On the other hand, it decreases drastically the quantum tunneling times, so that only solitons with sufficiently high velocities to separate from the quantum time-scale can move coherently for longer distances. Results showing the dependence of the "fast" mobility when varying the model parameters are summarized in the lower plot in Fig. 11. The whitest part corresponds to the optimal mobility regime, where the initially 2-site compacton-like soliton may travel for 10 sites before its maximum population expectation values at inter-site positions have decreased to 80% of their initial values. The sharp transition to a dark region when increasing Q_4 is a direct counterpart of the classical stability exchange: for larger Q_4, the ground-state is on-site rather than inter-site centered, and thus the initial state in this regime bears no resemblance to a 2-site compacton.

There are also alternative ways to construct localized quantum states which correspond to certain well-defined stationary states in the classical limit, such as the use of SU(f) coherent states (see, e.g., Ref. [5] for definition and discussion). As discussed in Ref. [36], we may describe a 2-site compacton as an SU(2) coherent state, then kick it by applying the phase operator, and use it as initial conditions for the quantum simulations analogously to above. The results are similar (the reader is referred to Ref. [36] for details), which shows that the conclusions above are not critically dependent on the specific choice of a quantum "compacton-like" initial state. One advantage with using the SU(f) construction is, that it works equally well in the regimes where the 2-site compacton is not the ground state. Thus, we could kick also an unstable 2-site SU(f) compacton and observe good large-velocity mobility close to the stability-exchange regime (essentially, we obtain a picture similar to the lower plot in Fig. 11 but without the sharp transition to the dark area in the upper part).

6 Conclusion

We hope the reader has enjoyed this brief review about the role of the concepts of PN potential and barrier for describing breather mobility, focusing mainly on the progress from the last 10-15 years on mobility of strongly localized modes, mobility in two-dimensional lattices, moving breathers in dissipative lattices with intrinsic gain, and mobility of strongly localized quantum breathers. We certainly did not make any attempt to give a complete review on the topic of moving breathers (that would in itself require a whole volume!), and we are aware of many important references that have been omitted. Instead, our main aim was to collect a number of different results which have previously appeared scattered in the literature into a common framework; although they address seemingly quite different physical systems such as the classical DNLS model with various modifications in 1D and 2D, flat-band modes, discrete Ginzburg-Landau models, and the quantum extended Bose-Hubbard model, they all share a central core of analyzing mobility of strongly localized modes in terms of the PN potential concept. Obviously, the description in terms of PN potentials is certainly not the only method needed in order to get a complete understanding of the very complex problem of moving breathers (in particular, the more mathematically oriented reader can be directed to Chapter 5 of Ref. [62] for a nice survey of various approaches used in more rigorous contexts). However, we might dare to say that without using these concepts, not much physical insight into the mechanisms by which localized excitations can be translated in any lattice (or, more generally, periodic potential) would have been reached. We are also certain that many more future applications will appear!

Acknowledgments

The main part of the work presented in Secs. 2-4 was performed by one of us (M.J.) in collaboration with, in chronological order, Michael Öster (Sec. 2), Rodrigo Vicencio (Secs. 3.1-3.2), Uta Naether (Sec. 3.1), and Jaroslaw Prilepsky and Stanislav Derevyanko (Sec. 4). M.J. is particularly grateful to the collaborators for producing the original versions of all figures, as well as the underlying numerical simulations, in Secs. 2-3. M.J. is also very grateful to Rodrigo Vicencio and Stanislav Derevyanko for their kind, repeated invitations to visit the Nonlinear Optics Group, Universidad de Chile, and the School of Engineering and Applied Science, Aston University, respectively, during which a large part of this work was realized. Much of the work presented here stems from original ideas of Serge Aubry and Sergej Flach, who are especially thanked by M.J. for many enlightening discussions on breather mobility. Among the many other colleagues who contributed with suggestions on various occasions, M.J. would like to give a special mentioning to Thierry Cretegny, from whom he first learned many of the intricate scenarios for breather mobility, and to Yaroslav Zolotaryuk for first pointing out to him the similarities with nontrivial PN potentials for kinks. Finally, Chris Eilbeck pioneered both topics of breather mobility and quantum breathers, and we are very grateful for many discussions during the years. Parts of this work were supported by the Swedish Research Council.

References

1. Arévalo, E.: Soliton Theory of Two-Dimensional Lattices: The Discrete Nonlinear Schrödinger Equation. Phys. Rev. Lett. **102**, 224102 (2009)
2. Aubry, S: Discrete Breathers: Localization and transfer of energy in discrete Hamiltonian nonlinear systems. Physica D **216**, 1 (2006)
3. Bergman, D.L., Wu, C., Balents, L.: Band touching from real-space topology in frustrated hopping models. Phys. Rev. B **78**, 125104 (2008)
4. Braun, O.M, Kivshar, Yu.S.: Nonlinear dynamics of the Frenkel-Kontorova model. Phys. Rep. **306**, 1 (1998)
5. Buonsante, P., Penna, V., Vezzani, A.: Attractive ultracold bosons in a necklace optical lattice. Phys. Rev. A **72**, 043620 (2005)
6. Butt, I.A., Wattis, J.A.D.: Discrete breathers in a two-dimensional Fermi-Pasta-Ulam lattice. J. Phys. A: Math. Gen. **39**, 4955 (2006)
7. Butt, I.A., Wattis, J.A.D.: Discrete breathers in a two-dimensional hexagonal Fermi-Pasta-Ulam lattice. J. Phys. A: Math. Gen. **40**, 1239 (2007)
8. Campbell, D.K., Peyrard, M.: Chaos and order in *non*integrable model field theories. Chaos, edited by D.K. Campbell (AIP, New York, 1990), p.305.
9. Champneys, A.R., Rothos, V.M., Melvin, T.R.O.: Travelling Solitary Waves in DNLS Equations. In Ref. [41], p. 379
10. Chong, C., Carretero-González, R., Malomed, B.A., Kevrekidis, P.G.: Multistable solitons in higher-dimensional cubic-quintic nonlinear Schrödinger lattices. Physica D **238**, 126 (2009)

11. Christiansen, P.L., Gaididei, Yu.B., Rasmussen, K.Ø., Mezentsev, V.K., Juul Rasmussen, J.: Dynamics in discrete two-dimensional nonlinear Schrödinger equations in the presence of point defects. Phys. Rev. B **54**, 900 (1996)
12. Cretegny, T: Dynamique collective et localisation de l'énergie dans les réseaux non-linéaires. Ph.D. Dissertation, École normale supérieure de Lyon, France, 1998
13. Cuevas, J., Eilbeck, J.C.: Discrete soliton collisions in a waveguide array with saturable nonlinearity. Phys. Lett. A **358**, 15 (2006)
14. Dauxois, T., Peyrard, M., Willis, C.R.: Discreteness effects on the formation and propagation of breathers in nonlinear Klein-Gordon equations. Phys. Rev. E **48**, 4768 (1993)
15. Dorignac, J., Eilbeck, J.C., Salerno, M., Scott, A.C.,: Quantum Signatures of Breather-Breather Interactions. Phys. Rev. Lett. **93**, 025504 (2004)
16. Dutta, O., Gajda, M., Hauke, P., Lewenstein, M., Lühmann, D.-S., Malomed, B.A., Sowiński, T., Zakrzewski, J.: Non-standard Hubbard models in optical lattice. arXiv:1406.0181v2 [cond-mat.quant-gas] 12 Jun 2014
17. Egorov, O.A., Lederer, F.: Spontaneously walking discrete cavity solitons. Opt. Lett. **38**, 1010 (2013)
18. Egorov, O.A., Lederer, F., Kivshar, Yu.S.: How does an inclined holding beam affect discrete modulational instability and solitons in nonlinear cavities? Opt. Express **15**, 4149 (2007)
19. Efremides, N.K., Christodoulides, D.N.: Discrete Ginzburg-Landau solitons. Phys. Rev. E **67**, 026606 (2003)
20. Eilbeck, J.C.: Numerical simulations of the dynamics of polypeptide chains and proteins. Computer Analysis for Life Science: Progress and Challenges in Biological and Synthetic Polymer Research, edited by C. Kawabata and A.R. Bishop, (Ohmsha, Tokyo, 1986), p. 12
21. Eilbeck, J.C.: Some Exact Results for Quantum Lattice Problems. Localization and Energy Transfer in Nonlinear Systems, Proceedings of the Third Conference, San Lorenzo de El Escorial Madrid, edited by L. Vázquez, R.S. MacKay, and M.P. Zorzano (World Scientific, Singapore, 2003), p.177
22. Eilbeck, J.C., Johansson, M.: The Discrete Nonlinear Schrödinger equation - 20 years on. Localization and Energy Transfer in Nonlinear Systems, Proceedings of the Third Conference, San Lorenzo de El Escorial Madrid, edited by L. Vázquez, R.S. MacKay, and M.P. Zorzano (World Scientific, Singapore, 2003), p.44
23. English, L.Q., Basu Thakur, R., Stearrett, R.: Patterns of travelling intrinsic localized modes in a driven electrical lattice. Phys. Rev. E **77**, 066601 (2008)
24. English, L.Q., Palmero, F., Sievers, A.J., Kevrekidis, P.G., Barnak, D.H.: Traveling and stationary intrinsic localized modes and their spatial control in electrical lattices. Phys. Rev. E **81**, 046605 (2010)
25. English, L.Q., Palmero, F., Stormes, J.F., Cuevas, J., Carretero-González, R., Kevrekidis, P.G.: Nonlinear localized modes in two-dimensional electrical lattices. Phys. Rev. E **88**, 022912 (2013)
26. Fischer, R., Träger, D., Neshev, D.N., Sukhorukov, A.A., Krolikowski, W., Denz, C., Kivshar, Yu.S.: Reduced-Symmetry Two-Dimensional Solitons in Photonic Lattices. Phys. Rev. Lett. **96**, 023905 (2006)
27. Falvo, C., Pouthier, V., Eilbeck, J.C.: Fast energy transfer mediated by multi-quanta bound states in a nonlinear quantum lattice. Physica D **221**, 58 (2006)
28. Flach, S., Gorbach, A.V.: Discrete breathers - Advances in theory and applications. Phys. Rep. **467**, 1 (2008)
29. Flach, S., Gorbach, A.V.: Discrete Breathers with Dissipation. Dissipative Solitons: From Optics to Biology and Medicine, N. Akhmediev and A. Ankiewicz (Eds.), Lecture Notes in Physics, Vol. 751 (Springer, Berlin, 2008), p.289
30. Flach, S., Willis, C.R.: Movability of Localized Excitations in Nonlinear Discrete Systems: A Separatrix Problem. Phys. Rev. Lett. **72**, 1777 (1994)
31. Flach, S., Willis, C.R.: Discrete breathers. Phys. Rep. **295**, 181 (1998)
32. Gómez-Gardeñes, J., Floría, L.M., Bishop, A.R.: Discrete breathers in two-dimensional anisotropic nonlinear Schrödinger lattices. Physica D **216**, 31 (2006)

33. Hadžievski, Lj., Maluckov, A., Stepić, M., Kip, D.: Power Controlled Soliton Stability and Steering in Lattices with Saturable Nonlinearity. Phys. Rev. Lett. **93**, 033901 (2004)
34. Jason, P.: Comparisons between classical and quantum mechanical nonlinear lattice models. Linköping Studies in Science and Technology. Thesis No. 1648 (Linköping, 2014); http://urn.kb.se/resolve?urn=urn:nbn:se:liu:diva-105817
35. Jason, P., Johansson, M.: Exact localized eigenstates for an extended Bose-Hubbard model with pair-correlated hopping. Phys. Rev. A **85**, 011603(R) (2012)
36. Jason, P., Johansson, M.: Quantum dynamics of lattice states with compact support in an extended Bose-Hubbard model. Phys. Rev. A **88**, 033605 (2013)
37. Jenkinson, M., Weinstein, M.I.: Vertex-, bond- and cell-centered bound states of the discrete nonlinear Schrödinger equation in dimensions 1, 2 and 3. arXiv:1405.3892v1 [nlin.PS] 15 May 2014
38. Johansson, M.: Discrete nonlinear Schrödinger approximation of a mixed Klein-Gordon/Fermi-Pasta-Ulam chain: Modulational instability and a statistical condition for creation of thermodynamic breathers. Physica D **216**, 62 (2006)
39. Johansson, M., Prilepsky, J.E., Derevyanko, S.A.: Strongly localized moving discrete dissipative breather-solitons in Kerr nonlinear media supported by intrinsic gain. Phys. Rev. E **89**, 042912 (2014)
40. Johansson, M., Sukhorukov, A.A., Kivshar, Yu.S.: Discrete reduced-symmetry solitons and second-band vortices in two-dimemsional nonlinear waveguide arrays. Phys. Rev. E **80**, 046604 (2009)
41. Kevrekidis, P.G.: The Discrete Nonlinear Schrödinger Equation: Mathematical Analysis, Numerical Computations and Physical Perspectives. STMP 232 (Springer, Berlin Heidelberg 2009)
42. Khare, A., Rasmussen, K. Ø., Samuelsen, M.R., Saxena, A.: Exact solutions of the saturable discrete nonlinear Schrödinger equation. J. Phys. A: Math. Gen. **38**, 807 (2005)
43. Kivshar, Yu.S., Campbell, D.K.: Peierls-Nabarro potential barrier for highly localized nonlinear modes. Phys. Rev. E **48**, 3077 (1993)
44. Kiselev, Al.S., Kiselev, An.S., Rozanov, N.N.: Dissipative Discrete Spatial Optical Solitons in a System of Coupled Optical Fibers with the Kerr and Resonance Nonlinearities. Opt. Spectrosc. **105**, 547 (2008)
45. Law, K.J.H., Saxena, A., Kevrekidis, P.G., Bishop, A.R.: Localized structures in kagome lattices. Phys. Rev. A **79**, 053818 (2009)
46. MacKay, R.S., Sepulchre, J.-A.: Effective Hamiltonian for travelling discrete breathers. J. Phys. A: Math. Gen. **35**, 3985 (2002)
47. Marín, J.L., Eilbeck, J.C., Russell, F.M.: Localized moving breathers in a 2D hexagonal lattice. Phys. Lett. A **248**, 225 (1998)
48. Marín, J.L., Falo, F., Martínez, P.J., Floría, L.M.: Discrete breathers in dissipative lattices. Phys. Rev. E **63**, 066603 (2001)
49. Melvin, T.R.O., Champneys, A.R., Kevrekidis, P.G., Cuevas, J.: Radiationless Travelling Waves In Saturable Nonlinear Schrödinger Lattices. Phys. Rev. Lett. **97**, 124101 (2006)
50. Mishmash, R.V., Danshita, I., Clark, C.W., Carr, L.D.: Quantum many-body dynamics of dark solitons in optical lattices. Phys. Rev. A **80**, 053612 (2009)
51. Molina, M.I.: Localized modes in nonlinear photonic kagome nanoribbons. Phys. Lett. A **376**, 3458 (2012)
52. Molina, M.I., Vicencio, R.A., Kivshar, Yu.S.: Discrete solitons and nonlinear surface modes in semi-infinite waveguide arrays. Opt. Lett. **31**, 1693 (2006)
53. Morgante, A.M., Johansson, M., Kopidakis, G., Aubry, S.: Standing wave instabilities in a chain of nonlinear coupled oscillators. Physica D **162**, 53 (2002)
54. Mozafari, E., Stafström, S.: Polaron dynamics in a two-dimensional Holstein-Peierls system. J. Chem. Phys. **138**, 184104 (2013)
55. Nabarro, F.R.N.: Dislocations in a simple cubic lattice. Proc. Phys. Soc. **59**, 256 (1947)
56. Naether, U., Vicencio, R.A., Johansson, M.: Peierls-Nabarro energy surfaces and directional mobility of discrete solitons in two-dimensional saturable nonlinear Schrödinger lattices. Phys. Rev. E **83**, 036601 (2011)

57. Naether, U., Vicencio, R.A., Stepić, M.: Mobility of high-power solitons in saturable nonlinear photonic lattices. Opt. Lett. **36**, 1467 (2011)
58. Öster, M.: Stability and Mobility of Localized and Extended Excitations in Nonlinear Schrödinger Models. Linköping Studies in Science and Technology. Dissertations No. 1072 (Linköping, 2007); http://urn.kb.se/resolve?urn=urn:nbn:se:liu:diva-8091
59. Öster, M., Johansson, M.: Stability, mobility and power currents in a two-dimensional model for waveguide arrays with nonlinear coupling. Physica D **238**, 88 (2009)
60. Öster, M., Johansson, M., Eriksson, A.: Enhanced mobility of strongly localized modes in waveguide arrays by inversion of stability. Phys. Rev. E **67**, 056606 (2003)
61. Peierls, R.: The size of a dislocation. Proc. Phys. Soc. **52**, 34 (1940)
62. Pelinovsky, D.E.: Localization in Periodic Potentials: From Schrödinger Operators to the Gross-Pitaevskii Equation. London Mathematical Society Lecture Note Series Vol. 390 (Cambridge University Press, Cambridge, 2011)
63. Peyrard, M., Remoissenet, M.: Solitonlike excitations in a one-dimensional atomic chain with a nonlinear deformable substrate potential. Phys. Rev. B **26**, 2886 (1982)
64. Pinto, R.A., Flach, S.: Quantum Discrete Breathers. Dynamical Tunneling: Theory and Experiment, edited by S. Keshavamurthy and P. Schlagheck, Chap. 14 (Taylor & Francis, Boca Raton, FL, 2011)
65. Russell, F.M.: Energy Gain by Discrete Particle Non-linear Lattice Excitations. Localized Excitations in Nonlinear Complex Systems: Current State of the Art and Future Perspectives, edited by R. Carretero-González, J. Cuevas-Maraver, D. Frantzeskakis, N. Karachalios, P. Kevrekidis, and F. Palmero-Acebedo (Springer, Cham, 2014), p. 289.
66. Savin, A.V., Zolotaryuk, Y., Eilbeck, J.C.: Moving kinks and nanopterons in the nonlinear Klein-Gordon lattice. Physica D **138**, 267 (2000)
67. Sepulchre, J.-A.: Energy barriers in coupled oscillators: from discrete kinks to discrete breathers. Localization and Energy Transfer in Nonlinear Systems, Proceedings of the Third Conference, San Lorenzo de El Escorial Madrid, edited by L. Vázquez, R.S. MacKay, and M.P. Zorzano (World Scientific, Singapore, 2003), p.102
68. Susanto, H., Kevrekidis, P.G., Carretero-González, R., Malomed, B.A., and Frantzeskakis, D.J.: Mobility of Discrete Solitons in Quadratically Nonlinear Media. Phys. Rev. Lett. **99**, 214103 (2007)
69. Vicencio, R.A., Johansson, M.: Discrete soliton mobility in two-dimensional waveguide arrays with saturable nonlinearity. Phys. Rev. E **73**, 046602 (2006)
70. Vicencio, R.A., Johansson, M.: Discrete flat-band solitons in the kagome lattice. Phys. Rev. A **87**, 061803(R) (2013)
71. Wang, W.Z., Tinka Gammel, J., Bishop, A.R., Salkola, M.I: Quantum Breathers in a Nonlinear Lattice. Phys. Rev. Lett. **76**, 3598 (1996)
72. Weinstein, M.I.: Excitation thresholds for nonlinear localized modes on lattices. Nonlinearity **12**, 673 (1999)
73. Yulin, A., Champneys, A.: Snake-to-isola transition and moving solitons via symmetry-breaking in discrete optical cavities. Disc. Cont. Dyn. Syst., Ser. S **4**, 1341 (2011)
74. Zhu, X., Wang, H., Zheng, L.-X.: Defect solitons in kagome optical lattices. Opt. Express **18**, 20786 (2010)
75. Zolotaryuk, Y., Christiansen, P.L., Juul Rasmussen, J.: Polaron dynamics in a two-dimensional anharmonic Holstein model. Phys. Rev. B **58**, 14305 (1998)